

## Investigation of 1-Phenyl-3-Methyl-5-Pyrazolone as a Corrosion Inhibitor for Mild Steel in 1M Hydrochloric Acid

Kun Cao<sup>1</sup>, Weihua Li<sup>2,\*</sup>, Lingmin Yu<sup>1</sup>

<sup>1</sup> College of Chemistry and Chemical Engineering, Key Laboratory of Marine Chemistry Theory and Technology, Ministry of Education, Ocean University of China, Qingdao 266100

<sup>2</sup> China Institute of Oceanology, Chinese Academy of Sciences, Qingdao 266071, China)

\*E-mail: [liweihua@qdio.ac.cn](mailto:liweihua@qdio.ac.cn)

Received: 10 October 2011 / Accepted: 28 November 2011 / Published: 1 January 2012

---

Corrosion inhibition efficiency of 1-phenyl-3-methyl-5-pyrazolone (PMP) as corrosion inhibitor on mild steel in acid solution was investigated by means of weight loss, potentiodynamic polarization curve, electrochemical impedance spectroscopy (EIS), raman spectrum and Quantum chemical method. Weight loss measurements gave an inhibition efficiency of about 32% in the presence of  $1 \times 10^{-5}$  M PMP, which increased to about 93% at PMP concentration of  $1 \times 10^{-3}$  M. EIS results revealed that PMP took effects excellently as a corrosion inhibitor for mild steel in 1 M hydrochloric acid media, and its efficiency attains more than 97.2% at  $1 \times 10^{-3}$  M at 298 K. Potentiodynamic polarization measurements showed that the presence of PMP in 1 M hydrochloric acid solutions decreased corrosion currents to a great extent. The above results showed that PMP acted as a mixed-type corrosion inhibitor, which was adsorbed on the steel surface via a coordination bond, giving rise to excellent corrosion inhibiting effect. The theoretical study by quantum chemical method was found that the active adsorption sites of PMP are phenyl and oxygen atom.

---

**Keywords:** Pyrazolone; Mild steel; Polarization curve; Electrochemical impedance spectroscopy; Quantum chemistry

### 1. INTRODUCTION

Hydrochloric acid is commonly used for removal of undesirable rust in the metal working, cleaning of boilers and heat exchangers [1,2]. To prevent unexpected metal reaction and excess acid consumption in the pickling processes of mild steel, inhibitors are added to the acid [3,4]. For many years, the use of inorganic salts and their blends, including chromates, nitrite, phosphonates, arsenic salts, have been found effective as corrosion inhibitor [5-7], but the major disadvantage is their toxicity [8]. These compounds generally form a protective film on the steel surface, which acts as a barrier to

aggressive media [9]. In general, organic compounds containing active elements including nitrogen, sulfur and oxygen [10-14], and heterocyclic compounds with polar functional groups and conjugated double bonds [15-18], have been reported to inhibit the corrosion of steel. Currently, the development of natural, non-toxic and novel corrosion inhibitors has been considered to be more important and desirable [19].

1-phenyl-3-methyl-5-pyrazolone (PMP) is commonly used to label the carbohydrates. This compound has nitrogen, oxygen in molecule, additionally, it is water-soluble. A perusal of literature reveals that PMP has not been investigated as corrosion inhibitor.

In this study, PMP is investigated as a new kind of environment-friendly inhibitor for the corrosion of mild steel in 1 M hydrochloric acid solution using electrochemical methods, weight loss test and quantum chemical calculation.

## 2. EXPERIMENT

PMP was dissolved in 1 M hydrochloric acid solution at various concentrations from  $1 \times 10^{-5}$  M to  $1 \times 10^{-3}$  M, and the 1 M hydrochloric acid solution without PMP was taken as blank for comparison.

The composition (wt %) of the mild steel was: Fe: 98.90; C: 0.18; Mn: 0.55; Si: 0.3; S: 0.034; P: 0.035. Specimens were mechanically cut into 5.00 cm $\times$ 2.50 cm $\times$ 0.4 cm (used in the weight loss experiment) and 1.0 cm  $\times$ 1.0 cm $\times$ 1.0 cm (used in the electrochemical experiment) dimensions, polished with SiC abrasive papers up to 800 grade, washed in distilled water, degreased ultrasonically in acetone, and dried at room temperature.

### 2.1 Electrochemical experiments

Electrochemical experiments were performed in a conventional three electrodes system, mild steels sealed by epoxy resin with exposure surface of 1 cm<sup>2</sup> as working electrodes, a platinum foil of 1.0 cm $\times$ 1.0 cm as counter electrode, and a saturated calomel electrode (SCE) provided with a Luggin capillary as reference electrode. Measurements were performed at room temperature with PARSTAT 2273 Electrochemical system.

EIS measurement was carried out on steady state open circuit potential (OCP) disturbed with amplitude of 10 mV a.c. sine wave at frequencies from 100 kHz to 10 mHz. Then the potentiodynamic polarization curves were obtained from  $-250$  mV (SCE) versus OCP to  $+250$  mV (SCE) versus OCP with a scan rate of 0.5 mV/s.

### 2.2 Weight loss experiment

Mild steel specimens in triplicate for each inhibitor concentration were immersed in the test acid solutions for 3 h at 298 K. After that, the specimens were scraped, rinsed in water and acetone, and dried in a desiccator. Finally, the loss in weight was determined with analytic balance.

### 2.3 SEM analysis

The surface morphology of specimens after immersed in 1M hydrochloric acid for 3 hour with and without inhibitors was obtained on a KYKY2800B scanning electronic microscope. The accelerating voltage was 25 kV.

### 2.4 Raman spectrum

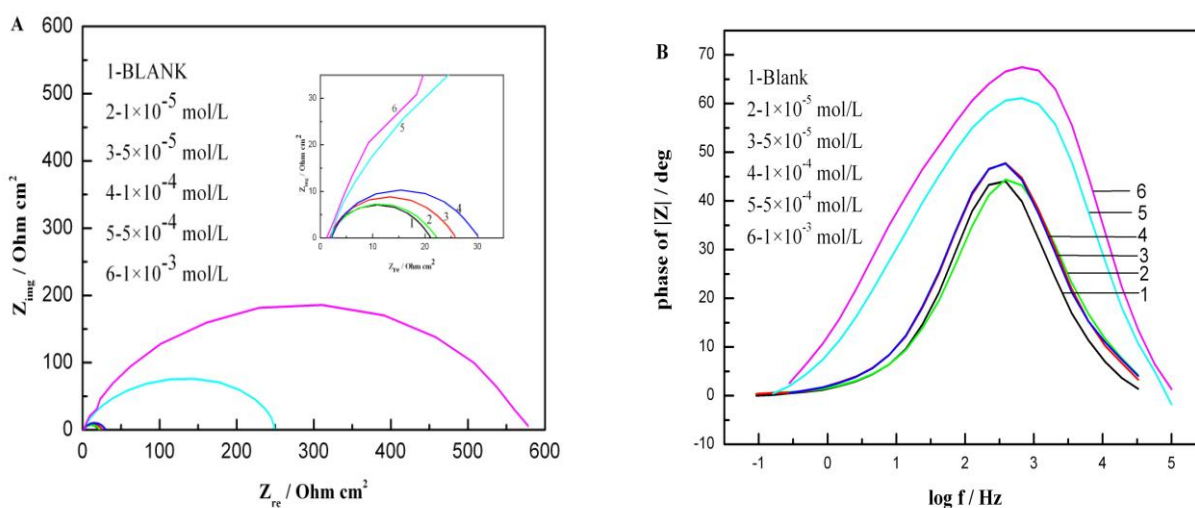
Raman spectra were measured using the microscope attachment of a Jobin Yvon Raman spectrometer operated in single spectrograph mode with a holographic dispersive grating of 1800 grooves/mm. Measurements of Raman were carried out on the steel surface after immersing in the 1M hydrochloric acid solution for 3 h. The metal surface was washed with distilled water and dried with steam nitrogen.

### 2.5 Quantum chemical calculation

In order to find out optimized conformations of the compounds studied and to speed up the calculations, the molecular structures were optimized initially with PM3 semi-experiential calculation [20]. The convergence was set to 0.01 kcal / mol.

## 3. RESULTS AND DISCUSSION

### 3.1 Electrochemical impedance spectroscopy (EIS)



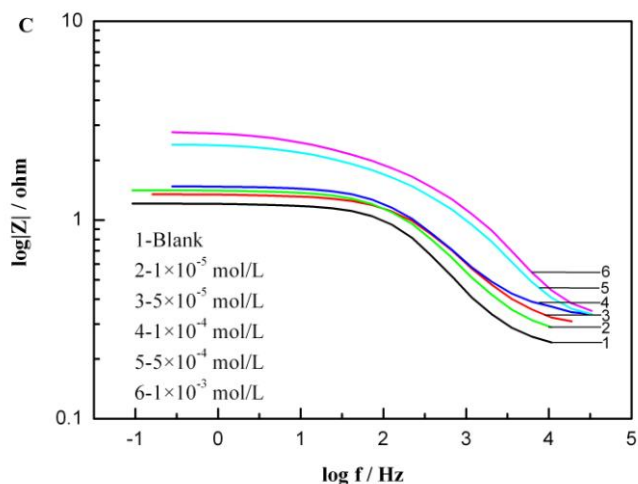


**Figure 1.** EIS plots of mild steel in 1M HCl with various concentrations of PMP

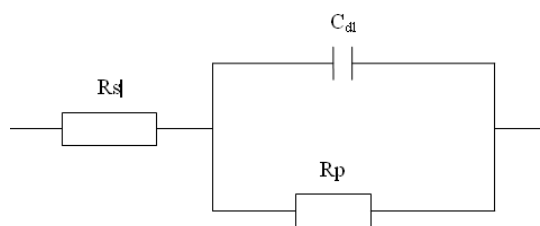


**Figure 2.** the equivalent circuit of the Nyquist plot

The electrochemical impedance spectroscopy provides important mechanistic and kinetic information for an electrochemical system under investigation. The inhibitive performance of various concentrations of PMP on mild steel immersed in 1M hydrochloric acid solution was studied via EIS at 298K. The impedance results were plotted in Fig.1. Impedance data were analyzed using the Zsimpwin ver. 3.21. The EIS parameters were calculated by analyzing the impedance plots fitting the equivalent circuit as mentioned in Fig.2, where  $R_s$  is the solution resistance,  $R_p$  is the polarization resistance and  $C_{dl}$  is the electrochemical double layer capacitance. The value of the parameters was tabulated in Table 1.

For EIS measurement, the inhibition efficiency ( $IE$ ) was calculated from the polarization resistance using Eq.1 [5].

$$IE\% = \frac{R_p - R_p^0}{R_p} \times 100 \dots\dots\dots (1)$$

$R_p$  and  $R_p^0$  are polarization resistances in the presence and absence of the inhibitors, respectively.

It is observed that increasing the concentration of PMP results in an increase in the impedance of the interface, which indicate inhibition of the corrosion process [21-23].  $C_{dl}$  values decrease with the increasing of inhibitor concentration.

**Table 1.** Impedance data of mild steel in 1M HCl with different concentrations of PMP

	Concentration (mol/L)	$R_s$ (ohm)	$10^5 C_{dl}$ (F·cm <sup>-2</sup> )	$R_p$ (ohm)	IE (%)
Blank	0	2.041	9.694	13.24	—
PMP	$1 \times 10^{-5}$	2.256	6.211	18.65	29.0
	$5 \times 10^{-5}$	2.093	5.909	22.22	40.4
	$1 \times 10^{-4}$	2.474	5.538	25.62	48.3
	$5 \times 10^{-4}$	2.483	5.933	212.9	93.8
	$1 \times 10^{-3}$	6.509	2.060	468.7	97.2

That is due to the gradual replacement of water molecules by the adsorption of the organic molecules at metal/solution interface, which leads to a protective film adsorbing on the metal surface.  $C_{dl}$  is expressed as

$$C_{dl} = \frac{\epsilon^0 \epsilon}{d} S \dots\dots\dots (2)$$

where  $d$  is the thickness of the film,  $S$  is the surface of the electrode,  $\epsilon^0$  is the permittivity of the air, and  $\epsilon$  is the local dielectric constant. According to Eq. 2, the decrease in  $C_{dl}$  can be explained by either the increase in the adsorption film area (which decreases the electrode surface area), the decrease in the local dielectric constant or the increase in the double layer thickness. Therefore, the diffusion of ions from the interface to the solution may be delayed and the dissolution reactions of mild steel may be inhibited to a great extent.

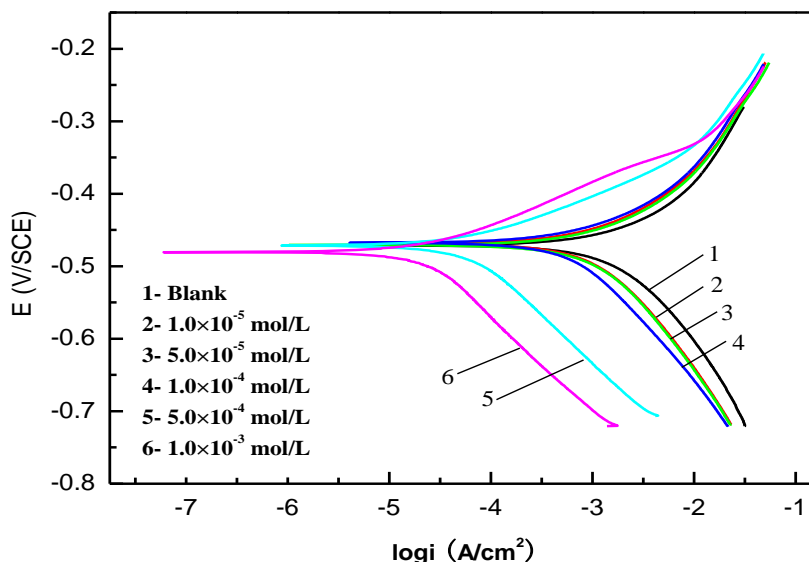
3.2 Polarization curve

Fig. 3 shows the typical polarization curves for the inhibition characteristics of PMP with different concentrations in 1M hydrochloric acid solution.

The anodic and cathodic current-potential curves are extrapolated up to their intersection at the point where corrosion current density ( $i_{corr}$ ) and corrosion potential ( $E_{corr}$ ) are obtained [7]. The electrochemical parameters  $E_{corr}$ ,  $i_{corr}$ , anodic and cathodic Tafel slopes ( $\beta_a$ ,  $\beta_c$ ) obtained from polarization measurements are listed in Table 2. The inhibition efficiency was calculated by Eq.3.[24]

$$IE\% = \frac{i_{corr}^0 - i_{corr}}{i_{corr}^0} \times 100 \dots\dots\dots (3)$$

where  $i_{corr}$  and  $i_{corr}^0$  are the corrosion current with and without inhibitor, respectively.



**Figure 3.** Polarization curves for mild steel in 1M HCl with different concentrations of PMP

**Table 2.** Polarization parameters and corresponding inhibition efficiencies for the corrosion of mild steel in 1M HCl with different concentrations of PMP

	Concentration (mol/L)	$E_{corr}$ (mV/SCE)	$i_{corr}$ ( $\mu\text{A}\cdot\text{cm}^{-2}$ )	$\beta_c$ ( $\text{mV}\cdot\text{dec}^{-1}$ )	$\beta_a$ ( $\text{mV}\cdot\text{dec}^{-1}$ )	IE (%)
Blank	0	-475	2.633	86.159	68.975	—
PMP	$1\times 10^{-5}$	-476	1.357	91.395	73.694	48.5
	$5\times 10^{-5}$	-472	1.250	92.896	79.042	52.5
	$1\times 10^{-4}$	-472	0.731	93.506	81.088	72.2
	$5\times 10^{-4}$	-474	0.613	93.539	84.731	76.7
	$1\times 10^{-3}$	-486	0.228	95.816	85.076	91.3

Addition of PMP greatly decreases the current density in Table 2. In addition, the  $E_{corr}$  values show slight shifts in negative directions. These effects are significantly enhanced upon increasing the PMP concentration.

As it can be seen from these polarization results, the  $i_{corr}$  values decrease considerably in the presence of PMP and decreased with increasing inhibitor concentration, and we notice that the inhibition efficiency increased with inhibitor concentration reaching a maximum value of 91.3% at  $10^{-3}$  M. Whereas, no definite trend was observed in the shift of  $E_{corr}$  values, in the presence of PMP in 1 M hydrochloric acid solutions. They act as corrosion inhibitors suppressing both anodic and cathodic reaction by adsorbed on the steel surface blocking the active sites [25], and there is no definite trend in the shift of  $E_{corr}$  values, it can be recognized as a classification evidence of the compounds is mixed-type inhibitors [2].

### 3.3 Weight loss measurements

Table 3 shows the weight loss values of mild steel in 1M hydrochloric acid solution in the absence and presence of various concentrations of PMP. The degree of surface coverage ( $\theta$ ) and the percentage inhibition efficiency are calculated via the following equations:

$$\theta = \frac{W_0 - W}{W_0} \dots\dots\dots (4)$$

$$IE_{(w)} = \frac{W_0 - W}{W_0} \times 100\% \dots\dots\dots (5)$$

where  $W_0$  and  $W$  are the weight losses of the test specimens in the absence and presence of the inhibitor, respectively.

**Table 3.** The results of weight loss experiment

	Concentration (mol L <sup>-1</sup> )	Corrosion rate (mg cm <sup>-2</sup> h <sup>-1</sup> )	IE (%)	$\theta$
Blank	0	0.6071	—	—
PMP	1.0×10 <sup>-5</sup>	0.4128	32	0.32
	5.0×10 <sup>-5</sup>	0.2495	58.9	0.589
	1.0×10 <sup>-4</sup>	0.1147	81.1	0.811
	5.0×10 <sup>-4</sup>	0.0923	84.8	0.848
	1.0×10 <sup>-3</sup>	0.0424	93.0	0.93

The inhibition efficiency of PMP calculated for 1.0×10<sup>-5</sup> M is about 32%, which increases to about 93% when the concentration of PMP increases to 1.0×10<sup>-3</sup>M. This is in good agreement with the values of  $IE$  obtained from EIS and polarization curves in 1M hydrochloric acid solution.

### 3.4 Adsorption isotherm

Basic information on the interaction between the inhibitor and the metal surface can be provided by the adsorption isotherm, which depends on the degree of electrode surface coverage ( $\theta$ ) obtained from the weight loss measurements with various concentrations of PMP at 298 K. We suppose that the adsorption of the inhibitor follows the Langmuir adsorption:

$$\frac{\theta}{1 - \theta} = k_{ads} C \dots\dots\dots (6)$$

where  $K_{ads}$  is adsorption equilibrium constant,  $C$  is the concentrations of PMP.

The best fitted straight line is obtained for the plot of  $C/\theta$  versus  $C$  with slope close to 1 (Fig. 4). The strong correlation ( $R=0.99916$ ) suggests that the adsorption of inhibitor on the metal surface obeys the Langmuir adsorption isotherm.[26]

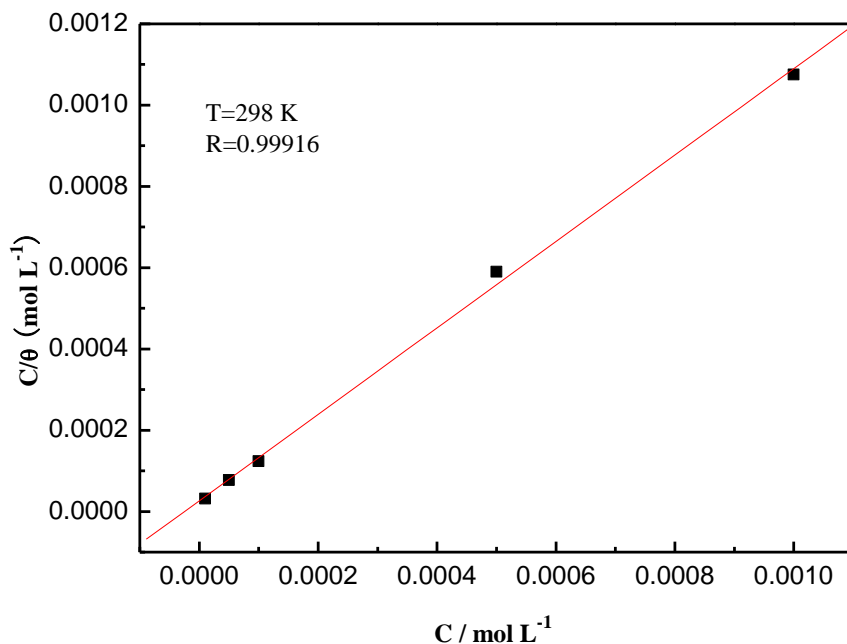


**Figure 4.** Adsorption isotherm for PMP on the surface of mild steel in 1M HCl

$K_{ads}$  values can be calculated, which is related to the standard free energy of adsorption  $\Delta G^0_{ads}$  through the following equations [1]:

$$K_{ads} = \frac{\theta}{C(1-\theta)} \dots\dots\dots (7)$$

$$k_{ads} = \left(\frac{1}{55.5}\right) \exp\left(\frac{-\Delta G^0_{ads}}{RT}\right) \dots\dots\dots (8)$$

The calculated  $\Delta G^0_{ads}$  value is  $-33.523 \text{ kJ}\cdot\text{mol}^{-1}$ , and the negative value indicates that the adsorption of PMP is a spontaneous process. The absolute values of  $\Delta G^0_{ads}$  are both around 33 kJ/mol. This confirms that the adsorption of PMP on copper surface may involve complex interactions: both physical adsorption and chemical adsorption [27].

The possible adsorption mechanism is [28]: (i) electrostatic interaction between the charged inhibitor molecules and charged steel surface.

This process is called physical adsorption, (ii) direct adsorption on the basis of donor-acceptor interactions between the lone pairs of electrons of heteroatoms, p-electrons of benzene and heterocyclic rings and the vacant orbitals of surface Fe atom.

This process is called chemical adsorption and (iii) indirect adsorption of the charged inhibitor molecules on the steel surface through a synergistic effect with  $H^+$  from 1M HCl solution, suggested that the adsorption of PMP on mild steel surface involve physical as well as chemical adsorption.

### 3.5 SEM analyses

The surface morphologies of the samples immersed in 1M hydrochloric acid solution are given in Fig.5. Fig.5(a) shows the SEM image in the absence of the inhibitor, showing that the mild steel surface is highly corroded with areas of localized corrosion. SEM image of the mild steel surface after immersed in 1M hydrochloric acid solution in the presence of 0.001 mol/L PMP is shown in Fig.5(b), where it can be seen that the rate of corrosion is suppressed, and there is little corrosion product on the steel surface.

This clearly reveals that there is a good inhibitor for the mild steel in 1M hydrochloric acid solution, decreasing the corrosion significantly.

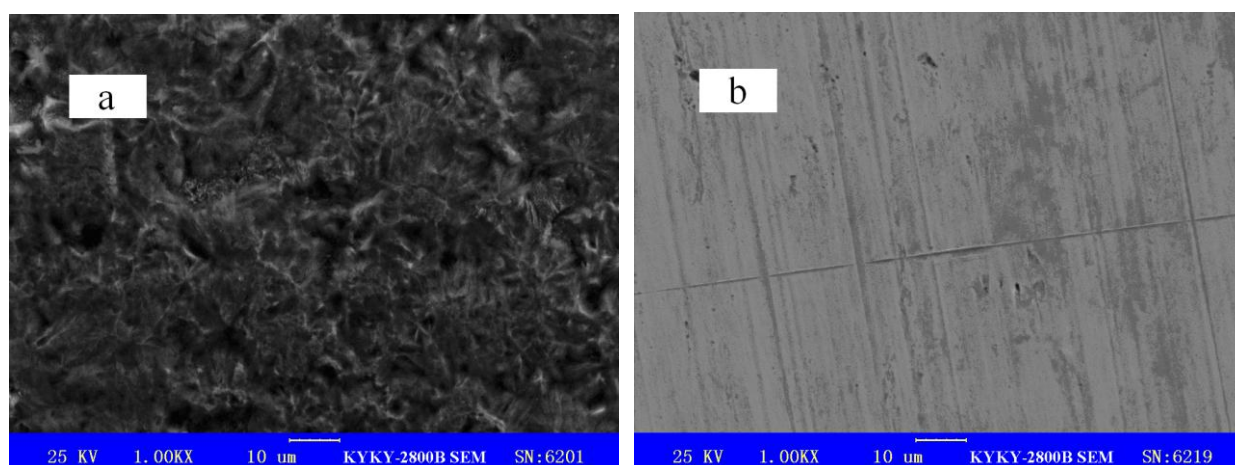


**Figure 5.** SEM images of the steel surfaces with and without inhibitors (a) without inhibitors, (b)with 0.001 mol/L PMP.

### 3.6 Raman spectrum

In order to confirm if the PMP molecules are indeed adsorbed onto the mild steel surface, we investigated the surface after immersion in the 1M hydrochloric acid solution for 3 h using Raman spectroscopy, as shown in Fig.6. The band at  $650.3\text{ cm}^{-1}$  belong to benzene ring out-of-plane stretching vibrations; the band at  $1700\text{ cm}^{-1}$  is belong to C=O stretching vibration; the C=N-N stretching vibration and N-N stretching vibration are found near  $1120$  and  $1201\text{ cm}^{-1}$ ; the three main bands at  $1243$ ,  $1450$  and  $1587\text{ cm}^{-1}$  are due to benzene ring stretching vibrations; the peak appearing at  $1610\text{ cm}^{-1}$  belong to C=N stretching vibration [29–32]. The characteristic bands found on the surface (Fig. 6) confirm the presence of PMP or its complex with mild steel in the formed film.

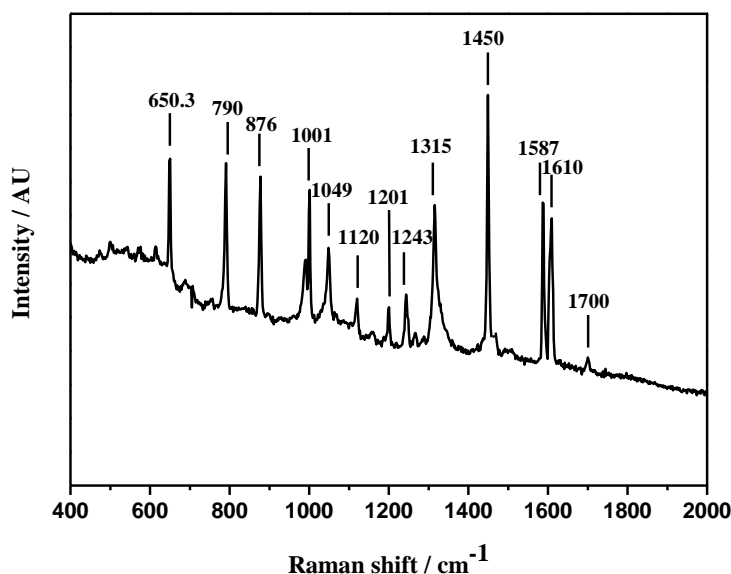


**Figure 6.** Raman spectrum of adsorption film formed on steel surface

### 3.7 Quantum chemical calculation

According to the frontier molecular orbital theory, the formation of a transition state is due to an interaction among frontier orbitals: high occupied molecular orbital (HOMO) and low unoccupied molecular orbital (LUMO) [33]. Thus, the treatment of the frontier molecular orbitals separately from the other orbitals is based on the general principles governing the nature of chemical reactions [33].  $E_{\text{HOMO}}$  is often associated with the donating ability of electron, and high value of  $E_{\text{HOMO}}$  is likely to indicate a strong tendency of the molecule to donate electron to appropriate electron-accepting molecules with low energy and empty molecular orbital, whereas  $E_{\text{LUMO}}$  indicates the ability to accept electron, and the lower values of  $E_{\text{LUMO}}$  show the more probability of the molecules to accept electrons [34]. Low absolute values of the energy band gap ( $\Delta E$ ) gives good inhibition efficiencies, meaning that the energy to remove an electron from the last occupied orbital will be low [34].

The optimized molecular structures of the studied molecules were obtained using PM3 semi-empirical calculation method and were shown in Fig. 7 and Fig. 8.

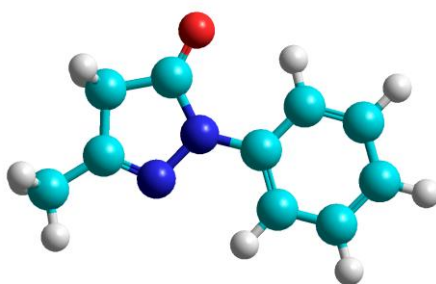


**Figure 7.** The optimized structure with PM3 semi-experience calculation

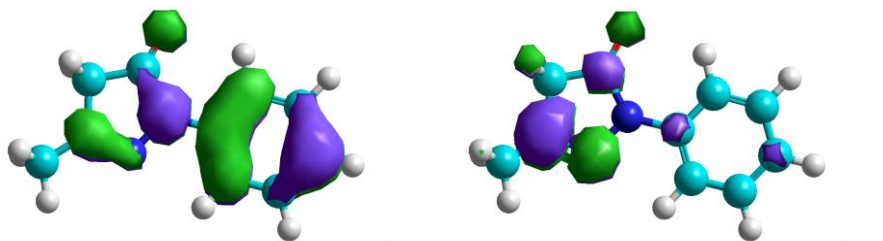


**Figure 8.** The HOMO and LUMO of PMP with PM3 semi-experience calculation

**Table 4.** Quantum chemical parameters of PMP

	$E_{HOMO}$	(eV)	$E_{LUMO}$	(eV)	$E_{HOMO}-E_{LUMO}$	$\mu$ (debye)
<b>PM3</b>	-8.635		-0.109		-8.526	3.974

The calculated quantum chemical parameters:  $E_{HOMO}$ ,  $E_{LUMO}$ ,  $\Delta E$  and dipole moment ( $\mu$ ) are presented in Table 4. Compared with the former works [35], the PMP had higher  $E_{HOMO}$ , indicating that it was easier to donate electron. According to the theoretical results and experiment data, it can be said that PMP was inclinable to get adsorbed on the metal surface.

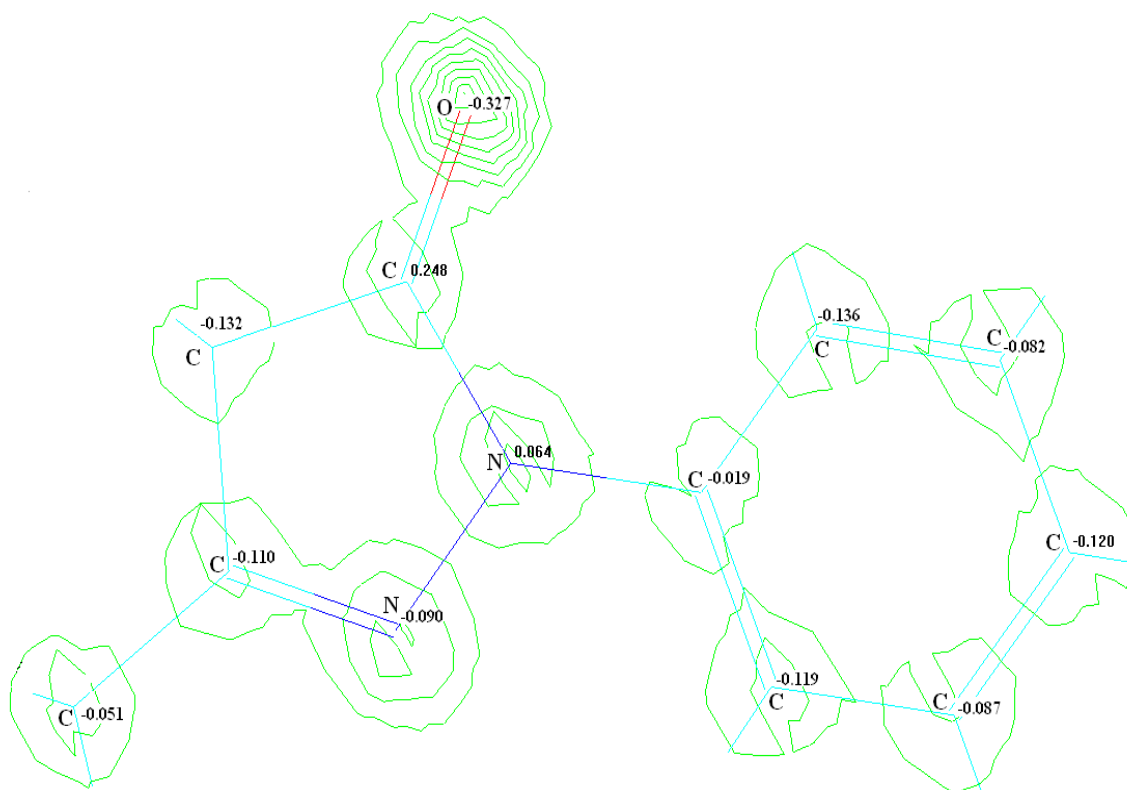


**Figure 9.** The charge density distribution of PMP

Fig. 9 shown the charge density distribution of PMP, and it is worth noticing that the more negative atom charges the adsorbed centre has, the more easily the atom donates its electrons to the unoccupied orbit of metal [36]. So the negative charges indicated that oxygen and carbon atoms in pyrazolone ring are the active adsorption site, as well as phenyl. The electronegativity of oxygen atom and the conjugated  $\pi$ -electron of the phenyl make them possible to form a coordination bond with iron surface. Nitrogen may also be an active site for its lone pair electron. According to the quantum chemical theory and the experimental results, it can be concluded that PMP has inclination to get adsorbed on the metal surface.

#### 4. CONCLUSION

(1) The electrochemical tests indicate that PMP behaves mainly as mixed-type inhibitor, and the IE% increased with increasing the concentration and reached the highest value at 0.001 M.

(2) The results obtained from weight loss test and electrochemical measurements were in good agreement, the adsorption model obeyed the Langmuir adsorption isotherm, and the adsorption of PMP is a spontaneous process.

(3) PMP molecule is connected with the iron atom via its O atom, C atom and phenyl.

#### References

1. T. Y. Soror, H. A. El-Dahan and N. G. El-Sayed Ammer, *J. Mater. Sci. Technol.*, 15 (2009) 559.
2. H. Ashassi-Sorkhabi, M. R. Majidi and K. Seyyedi, *Appl. Surf. Sci.*, 225 (2004) 176.
3. S. A. Abd El-Maksoud and A. S. Fouda, *Mater. Chem. Phys.*, 93 (2005) 84.
4. A. Chetouani, K. Medjahed and K. E. Benabadji, *Prog. Org. Coat.*, 46 (2003) 312.
5. W. H. Li, Q. He, C. L. Pei and B. R. Hou, *Electrochim. Acta*, 52 (2007) 6386.
6. M. Rohwerder and A. Michalik, *Electrochim. Acta*, 53 (2007) 1300.
7. K. Khaled, *Electrochim. Acta*, 48 (2003) 2493.
8. F. Bentiss, M. Traisnel, L. Gengembre and M. Lagrenée, *Appl. Surf. Sci.*, 152 (1999) 237.
9. V. Lakshminarayanan, R. Kannan and S. R. Rajagopalan, *J. Electroanal. Chem.*, 364 (1994) 79.
10. H. Ma, S. Chen, L. Niu, S. Zhao, S. Li and D. Li, *J. Appl. Electrochem.*, 32 (2002) 65.
11. H. Otmacic, J. Telegdi, K. Papp and E. J. Stupnisek-Lisac, *J. Appl. Electrochem.*, 34 (2004) 545.
12. D. Q. Zhang, L. X. Gao and G. D. Zhou, *Appl. Surf. Sci.*, 225 (2004) 287.
13. A. G. Christy, A. Lowe, V. O. Alego and M. Stoll, *J. Appl. Electrochem.*, 34 (2004) 225.
14. F. G. Zucchi, Trabanelli and M. Fonsati, *Corros. Sci.*, 38 (1996) 2019.
15. H. Otmacic and E. Stupnisek-Lisac, *Electrochim. Acta*, 48 (2002) 985.
16. M. A. Elmorsi and A. M. Hassanein, *Corros. Sci.*, 41 (1999) 2337.
17. M. Scendo, D. Poddebniak and J. Malyszko, *J. Appl. Electrochem.*, 33 (2003) 287.
18. F. M. Al-Kharafi, *Corros. Sci.*, 28 (1988) 163.
19. J. Sinko, *Prog. Org. Coat.*, 42 (2001) 267.
20. J. J. P. Stewart, *J. Comput. Chem.*, 10 (1989) 209.
21. H. Ashassi-Sorkhabi and N. Ghalebsaz-Jeddi, *Electrochim. Acta*, 51 (2006) 3848.
22. K. Juttner, *Electrochim. Acta*, 35 (1990) 1501.
23. W. R. Fawcett, Z. Kovacova, A. Motheo and C. Foss, *J. Electroanal. Chem.*, 91 (1992) 326.
24. S. S. A. El-Rehim, A. M. M. Ibrahim and F. F. Khaled, *J. Appl. Electrochem.*, 29 (1999) 593.

25. B. Gao, X. Zhang and Y. Sheng, *Mater. Chem. Phys.*, 108 (2008) 379.
26. A. S. Algaber and E. M. El-Nemma, *Mater. Chem. Phys.*, 86 (2004) 26.
27. W. H. Li, Q. He, S. T. Zhang, C. L. Pei and B. R. Hou, *J. Appl. Electrochem.*, 38 (2008) 289.
28. I. Ahamad, R. Prasad and M. A. Quraishi, *Corros. Sci.*, 52 (2010) 933.
29. E. M. sheriff, R. M. Erasmus and J. D. Comins, *Corros. Sci.*, 50 (2008) 3439.
30. C. S. Allen and R. P. Van Duyne, *Chem. Phys. Lett.*, 63 (1979) 455.
31. X. Gao, J. P. Davis and M. J. Weaver, *J. Phys. Chem.*, 94 (1990) 6858.
32. M. Moskovitz and J. S. Suh, *J. Phys. Chem.*, 88 (1990) 1986.
33. G. Gece and S. Bilgic, *Corros. Sci.*, 51 (2009) 1876.
34. G. Gece, *Corros. Sci.*, 50 (2008) 2981.
35. Y. Yan, W. H. Li, L. K. Cai and B. R. Hou, *Electrochim. Acta*, 53 (2008) 5953.
36. C. T. Wang, S. H. Chen, H. Y. Ma and C. S. Qi, *J. Appl. Electrochem.*, 33 (2003) 179.